anthracene. Recrystallization from benzene/hexane mixture produced yellow crystals: mp 180–182 °C; ^{1}H NMR ($CDCl_3$) 3.15 (s, 3 H), 7.23–7.77 (m, 7 H), 7.82–7.87 (m, 4 H), 8.31–8.40 (m, 2 H); MS, see Table IV.

10-Hydroxy-10-methyl-9-anthrone (13). The procedure of Julian, Cole, and Diemer was used.[28] A solution of methylmagnesium iodide in ether (100 mmol) was added to a suspension of anthraquinone (200 mmol) in 300 mL of benzene under argon. After the workup, yellow crystals were obtained upon recrystallization from benzene/hexane: mp 159–161 °C; ^{1}H NMR ($CDCl_3$) 1.66 (s, 3 H), 2.72 (s, 1 H), 7.2–8.2 (m, 8 H); MS, see Table IV.

10-Methyleneanthrone (14). This compound prepared by stirring 9-hydroxy-9-methyl-10-anthrone in a boiling mixture of oxalic and acetic acids for 45 s:[29] mp 147–149 °C; ^{1}H NMR ($CDCl_3$) 6.33 (s, 2 H), 7.25–7.67 (m, 4 H), 7.95–7.99 (m, 2 H), 8.05–8.41 (m, 2 H); MS, see Table IV.

9,10-Dihydroxyanthracene. This compound was prepared according to the method of Dimmel et al.:[30] MS of the bis(trimethylsilyl) ether, see Table IV.

General Procedure for Oxidations. In a typical reaction appropriate amounts of the acylanthracene and perchloric acid were added to an acetonitrile/water (70/30) mixture to form solutions of desired concentrations. After refluxing for 10 min under argon, stock solutions of copper(II) perchlorate and peroxydisulfate were added respectively to the rapidly stirred reactants. At the chosen time, reactions were quenched with water, internal standard was added, and the mixtures were extracted with three 15-mL volumes of CH_2Cl_2. The extracts were combined and dried over $MgSO_4$. When silylation was employed to derivatize anthrols and hydroxyanthrones, 3–5 drops of the above solutions were mixed with 1 drop of pyridine followed by the addition of 100 μL of *N,O*-bis(trimethylsilyl)acetamide (BSA). Analyses of the samples were accomplished within 1 h of silylation as storage for long periods of time caused decomposition.

Kinetic Determinations. Reactions (Table II) were initiated by addition of a 0.2-mL aliquot of a solution, 0.02–0.05 M acylanthrone or anthrone, and 0.05 M phenanthrene to a 20-mL volume of reactants at specific concentrations (Table III) and at reflux under Ar. At periodic intervals 1-mL aliquots of the reacting solution were withdrawn, diluted with 2 mL of water and shaken with 2–5-mL portions of methylene chloride. The extracts were dried over anhydrous sodium sulfate and analyzed by GC. A natural log plot of the area ratios of reactants to phenanthrene vs. time yielded pseudo-first-order rate constants for the reactions. The decrease in reactant was usually followed for two or more half-lives.

Product Identifications and Analyses. Products were usually identified by matching capillary GC retention times and capillary GC–MS spectra with authentic standards. For instances when authentic standards could not be obtained identifications were based on interpretations of the GC–MS spectra (see Table IV). GC response factors to phenanthrene internal standard were determined for anthracene, anthrone, anthraquinone, acetylanthracene, benzoylanthracene, anthracenecarboxaldehyde, 10-hydroxy-10-methylanthrone, and the trimethylsilyl ether of anthrol. Response factors for the other products were estimated from the response factors of these compounds.

Registry No. **1a**, 642-31-9; **1b**, 784-04-3; **1c**, 1564-53-0; **2**, 90-44-8; **3**, 84-65-1; **6** (R = CH_3), 98540-92-2; **6** (R = Ph), 53010-87-0; **6a**, 85090-11-5; **8** (R = CH_3), 98540-93-3; **8** (R = Ph), 98540-94-4; **10** (R = H), 7072-00-6; **10** (R = Ph), 24451-23-8; **12**, 17104-31-3; **13**, 4159-04-0; **14c** (trimethylsilyl deriv), 98540-99-9; PhCOCl, 98-88-4; CH_3CO_2H, 64-19-7; $PhCO_2H$, 65-85-0; $NH_3 \cdot (OSO_2OH)_2$, 7727-54-0; anthracene, 120-12-7; 9-anthrol trimethylsilyl ether, 28871-54-7; 9-methylanthracene, 779-02-2; 9,10-dihydroxyanthracene bis(trimethylsilyl ether), 28871-52-5; 10-hydroxy-10-acetyl-9-anthrone trimethylsilyl ether, 98540-95-5; 10-acetoxy-9-anthrol trimethylsilyl ether, 98540-96-6; 10-benzoyl-9-anthrol trimethylsilyl ether, 98540-97-7; 10-hydroxy-10-benzoylanthrone trimethylsilyl ether, 98540-98-8.

(28) Julian, P. L.; Cole, W.; Diemer, G. *J. Am. Chem. Soc.* **1945**, *67*, 1721. Bhattacharya, A. K.; Miller, B. *J. Org. Chem.* **1983**, *48*, 2412.
(29) Heymann, H.; Trowbridge, L. *J. Am. Chem. Soc.* **1950**, *72*, 84.
(30) Dimmel, D. R.; Shepard, D. *J. Org. Chem.* **1982**, *47*, 22.

Alkylation of Ambident Anions Derived from 2-Aryl-1,3,4-oxadiazol-5(4*H*)-ones. 1. Crystal Structures of the Silver and Rubidium Salts of 2-Phenyl-1,3,4-oxadiazol-5(4*H*)-one

Michèle Dessolin,[†] Michel Golfier,*[†] and Thierry Prangé[‡]

Laboratoire de Chimie Organique de Synthèse, Bâtiment 420, Université de Paris-Sud, 91405 Orsay Cedex, France, and LURE, Bâtiment 209 C, Université de Paris-Sud, 91405 Orsay Cedex, France

Received April 16, 1985

The analyses of crystal structures of two 2-phenyl-1,3,4-oxadiazol-5(4*H*)-one salts (Rb^+ and Ag^+) indicate an excellent agreement between the steric influence of the cation and the chemical behavior of the salts upon heterogeneous alkylation. This provides the first experimental structural evidence of a shielding effect induced by the cation over the possible alkylation sites of the anion. This effect controls the regioselectivity of the O- vs. N-alkylation and explains the different behavior of silver salt vs. alkaline salts under heterogeneous conditions.

The alkylation of anionic species derived from amide salts (termed "ambident anions" thereafter[1]) are known to follow different pathways depending on now quite well-defined factors.[2] Two of them are known to play a key role in the reaction: (1) the nature of the counterion and (2) the homogeneous or heterogeneous state of the reaction, in connection with the solvent used.

These factors have been widely investigated in the case of alkylation of 2-pyridone,[3] 2- and 4-hydroxypyrimidine,[4] and formanilide[5] salts. All these salts are true ambident anions with two possible alkylation sites. In the present

[†] Laboratoire de Chimie Organique de Synthèse.
[‡] LURE.

(1) Kornblum, N.; Smiley, R. A.; Blackwood, R. K.; Iffland, D. C. *J. Am. Chem. Soc.* **1955**, *77*, 6269–6280.
(2) (a) Gompper, R. *Angew. Chem., Int. Ed. Engl.* **1964**, *3*, 560–570. (b) Gompper, R.; Wagner, H. U. *Angew. Chem., Int. Ed. Engl.* **1976**, *15*, 321–331. (c) LeNoble, W. J. *Synthesis* **1970**, 1–6.
(3) (a) Hopkins, G. C.; Jonak, J. P.; Minnemeyer, H. J.; Tieckelmann, H. *J. Org. Chem.* **1967**, *32*, 4040–4044. (b) Chung, N. M.; Tieckelmann, H. *J. Org. Chem.* **1970**, *35*, 2517–2520.
(4) (a) Hopkins, G. C.; Jonak, J. P.; Tieckelmann, H.; Minnemeyer, H. J. *J. Org. Chem.* **1966**, *31*, 3969–3973. (b) Jonak, J. P.; Hopkins, G. C.; Minnemeyer, H. J.; Tieckelmann, H. *J. Org. Chem.* **1970**, *35*, 2512–2516.

0022-3263/85/1950-4461$01.50/0

Scheme I

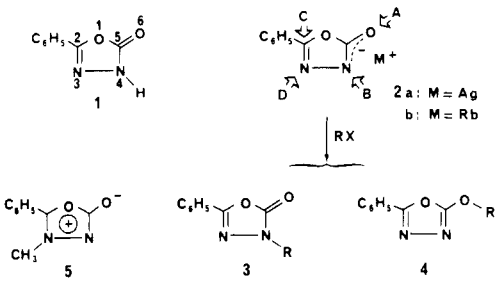

study, we investigate the case of 2-phenyl-1,3,4-oxadiazol-5(4*H*)-one (**1**), a model which was initially expected to be alkylated at four different positions of the heterocyclic part of the molecule. Three of the corresponding alkylation products have been previously obtained by us.[6,7] The four sites of alkylation a priori allowed (**2**, sites A–D) are given in the Scheme I.

The results of the alkylation of **2** under various conditions can be summarized as follows. (1) C(2) carbon alkylation was never observed, though the corresponding derivatives are known[8] but are very unstable. (2) For homogeneous reactions, alkylation occurs solely on the N(4) nitrogen, whatever may be the associated cation. The thermodynamically more stable product **3** is isolated as the single product of the reaction. (3) For heterogeneous reaction (solvent CH_2Cl_2) the following obtain: (a) All the alkali metal salts (M = Li to Cs) are unreactive. (b) The silver salt is mainly alkylated on the O(6) atom, to yield imidate **4**. A small amount of N(4)-alkylated product **3** is also formed. Upon varying the solvent, it is seen that the more soluble the silver salt is, the more N(4)-alkylated product **3** obtained. This strongly suggests, in accordance with similar results on 2-pyridone,[3] 2- and 4-hydroxypyrimidines,[4] and especially with formanilides,[5] that the heterogeneous reaction gives exclusively the O-alkylation, whereas the N-alkylation results from the small part of the reaction which occurs in solution and cannot be completely avoided. (c) With the silver salt, when using methyl iodide as the alkylating reagent, the product of N(3)-alkylation (isosydnone **5**) is also obtained in quite high yields (up to 37%) along with **4** (51%) and **3** (12%).

Despite an apparent complex behavior, and if we except the special case of methyl iodide in heterogeneous reaction, the oxadiazolone model we selected gives the same reactions as ordinary amide ambident anions.

A major approach of the heterogeneous reaction mechanism using solid or crystalline salts has been made in 1959 by Kornblum and Lurie[9] (for C- vs. O-alkylation and N- vs. O-alkylation) and by Stein and Tan[5] (for N- vs. O-alkylation). To explain the apparent discrepancies in the regioselectivity of the reaction, they proposed a masking effect of the cation upon the anionic part of the salt as the leading effect governing the selectivity and the orientation of the alkylation.

Up to now, this hypothesis has not received any confirmation by solid-state analysis of the different salts involved as substrates in the reaction. For these reasons, we have investigated by single-crystal X-ray techniques the structures of the silver and rubidium salts of 2-phenyl-1,3,4-oxadiazol-5(4*H*)-one (**2a**, M = Ag; **2b**, M = Rb). The potassium salt was a priori a better choice, since the K^+ ionic radius (1.33 Å) is closer to the Ag^+ ionic radius (1.26 Å) than is that of Rb^+ (1.48 Å). However all attempts to prepare single-crystals of the potassium salt failed, and only a microcrystalline powder was obtained, in spite of numerous trials.

Table I. Crystal Data and Details of Refinement for the Ag^+ and Rb^+ Salts

	Ag^+	Rb^+
system	monoclinic	orthorhombic
space group	$P2_1/c$	*Pbca*
parameters		
a, Å	8.395 (4)	35.310 (9)
b, Å	18.256 (4)	7.466 (8)
c, Å	7.058 (2)	6.744 (5)
β, deg	111.7	
number of structural factors (with $I > 2\sigma(I)$)	1084 (Mo Kα) 1192 (Cu Kα)	955 (Cu Kα)
final R^a %	5.3 (Mo Kα) 4.1 (Cu Kα)	6.3 (Cu Kα)
R_w, %	5.1 (Mo Kα) 5.5 (Cu Kα)	6.6 (Cu Kα)

[a] See ref 10.

Experimental Section

Both Ag^+ and Rb^+ salts crystallize as small cubes from NH_4OH aqueous solution, on cooling (Ag^+), or from a mixture of ethyl acetate/2-methylpentane-2,4-diol (Rb^+). These crystals were found stable at room temperature and in daylight, an exceptional behavior for a silver salt. Samples of 0.4 × 0.4 × 0.4 mm and 0.2 × 0.2 × 0.1 mm in size were selected for the Ag^+ and Rb^+ salts, respectively. They were mounted on a Philips PW 1100 four-circle diffractometer operating with the Cu Kα radiation (λ = 1.5418 Å) monochromated by graphite. In the case of the Ag^+ salt, a second recording was made by using the Mo Kα radiation (λ = 0.7158 Å). In each case, the orientation matrices were calculated from the angular settings of 25 randomly distributed reflections found in the range $10° < \theta < 25°$ and refined by a least-squares procedure. No significant decomposition was found in both cases and no correction was applied. The crystal data and parameters are reported in Table I. The intensities were reduced to *F* factors by means of standard Lorentz and polarization corrections and considered as observed above the 2σ background level.

Resolution and Refinements. In the two structures, the position of the heavy atom was easily deduced from the corresponding Patterson maps. The rest of the light atoms were obtained after subsequent Fourier difference syntheses. The data were corrected from absorption, by using the method described by Walkers,[11] at the end of the isotropic refinements. In the Ag^+ salt structure, two molecules of water were located in the packing. The refinements were carried out by full-matrix least squares with anisotropic thermal factors for all the non-hydrogen atoms. The hydrogen atoms were deduced from Fourier difference maps and kept at their places with an isotropic thermal factor equal to that of the bonded carbon. In the case of the Ag^+ salt, careful analysis of the electronic density as well as the hydrogen distribution, is in favor of water (two hydrogens) rather than ammonia (three hydrogens) as solvating molecules. At the end of the refinements, Fourier difference maps indicated that no peak greater than 0.5 e/Å^3 were present, except some spurious densities around the heavy atoms. No significant differences in bond lengths and angles were found in the two recordings at different wavelengths for the Ag^+ salt structure. The following discussion will concern only the set that gives the best *R* value (Mo Kα recording). The refinement converged to the final *R* value[10] given in Table I. The

(5) Stein, A. R.; Tan, S. H. *Can. J. Chem.* **1974**, *52*, 4050–4061.
(6) Golfier, M.; Milcent, R. *Bull. Soc. Chim. Fr.* **1973**, 254–258.
(7) Dessolin, M.; Golfier, M., to be published.
(8) Lee, S. L.; Gubelt, G. B.; Cameron, A. M.; Warkentin, J. *J. Chem. Soc., Chem. Commun.* **1970**, 1074–1075.
(9) Kornblum, N.; Lurie, A. P. *J. Am. Chem. Soc.* **1959**, *81*, 2705–2710.
(10) The *R* values are defined as $R = \sum||F_o| - |F_c||/\sum|F_o|$ and $R_w = (\sum w(|F_o| - |F_c|)^2/\sum w(F_o)^2)^{1/2}$, where *w* is the weight given for each reflection. The weights were $1/(\sigma(F_o))^2$, being deduced from counting statistics.
(11) Walkers, N.; Stuart, D. *Acta Crystallogr., Sect. A* **1983**, *A39*, 158–162.

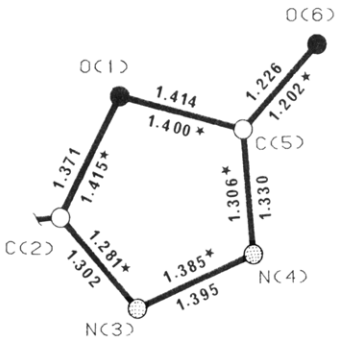

Figure 1. Bond distances measured after refinements in the oxadiazolone rings of Ag^+ and Rb^+ salts (starred values are those of Rb^+ salt).

Table II. Positional Parameters ($\times 10^4$) and Mean Recalculated Isotropic Thermal Factors ($\times 10^4$) for the Non-Hydrogen Atoms (esd's in Parentheses)

atom	fractional coordinates X	Y	Z	⟨U⟩
		Ag^+ Salt (Mo Kα)		
Ag	8701 (1)	10888 (1)	5481 (1)	33 (1)
O(1)	3471 (8)	10490 (4)	1872 (10)	28 (8)
C(2)	4212 (12)	9821 (6)	1875 (15)	28 (12)
N(3)	5845 (10)	9815 (5)	2976 (13)	33 (10)
N(4)	6222 (11)	10523 (5)	3763 (13)	32 (11)
C(5)	4823 (13)	10938 (6)	3126 (15)	32 (12)
O(6)	4547 (10)	11575 (4)	3462 (12)	45 (10)
C(7)	3161 (12)	9230 (6)	742 (15)	29 (11)
C(8)	1448 (13)	9365 (6)	−513 (16)	38 (12)
C(9)	421 (14)	8796 (7)	−1611 (18)	40 (15)
C(10)	1065 (15)	8100 (7)	−1504 (20)	41 (16)
C(11)	2786 (16)	7956 (7)	−287 (22)	52 (17)
C(12)	3817 (14)	8534 (6)	846 (18)	39 (14)
W(1)	11241 (12)	11238 (6)	7182 (15)	51 (13)
W(2)	2693 (10)	12445 (5)	5322 (12)	49 (11)
		Rb^+ Salt		
Rb	−334 (1)	695 (2)	2702 (2)	33 (1)
O(1)	931 (2)	1646 (11)	2042 (13)	24 (10)
C(2)	1059 (4)	172 (19)	3175 (19)	29 (17)
N(3)	799 (3)	−1012 (14)	3360 (17)	27 (14)
N(4)	486 (3)	−437 (14)	2301 (18)	23 (13)
C(5)	561 (4)	1136 (18)	1551 (19)	21 (16)
O(6)	369 (3)	2166 (12)	620 (12)	25 (11)
C(7)	1444 (4)	179 (20)	3918 (19)	26 (17)
C(8)	1551 (4)	−1138 (22)	5220 (23)	47 (21)
C(9)	1923 (4)	−1201 (25)	5896 (27)	57 (24)
C(10)	2184 (5)	48 (28)	5277 (25)	51 (24)
C(11)	2078 (4)	1379 (23)	3946 (22)	39 (20)
C(12)	1709 (4)	1449 (22)	3293 (22)	34 (18)

coordinates and the mean isotropic U factor, calculated from anisotropic parameters as $\langle U \rangle = {}^1/_3[u_{11} + u_{22} + u_{33} + 2(u_{12} \cos \gamma + u_{13} \cos \beta + u_{23} \cos \alpha)]$, are given in Table II. The intramolecular bond distances and angles deduced from these coordinates are depicted in Figure 1, for the heterocyclic ring only (i.e., the focused part of the molecule).

Results and Discussion

A close inspection of the bond distances (Figure 1) indicates that some electronic localization is present in the heterocyclic part of the molecule: C(5)–N(4) and N(3)–C(2) distances are somewhat shorter than the central N(4)–N(3) bonds. As deduced from Figure 1, no particular differences between the two salts can be noticed in the oxadiazolone ring, as bond length differences lie within their esd's.

The orientation of the phenyl group with respect to the oxadiazolone ring is the same in the two structures: The dihedral angles are 8.1° and 11° for the Ag^+ and Rb^+ salts, respectively.

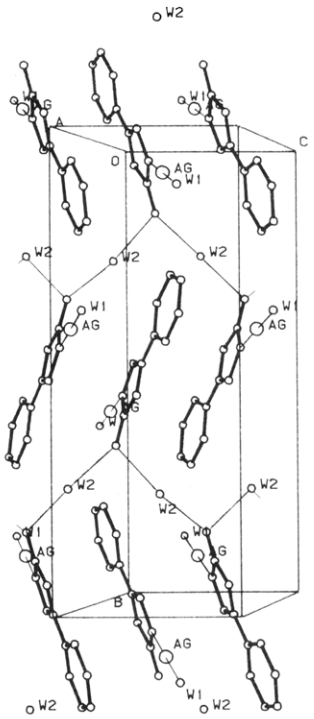

Figure 2. Ball-and-stick drawing of the packing of Ag^+ salt. (For purpose of clarity, metal atoms are represented by large open circles, and the others (C, N, O) by small open circles. Only the metal atom and the solvating molecules are labeled.)

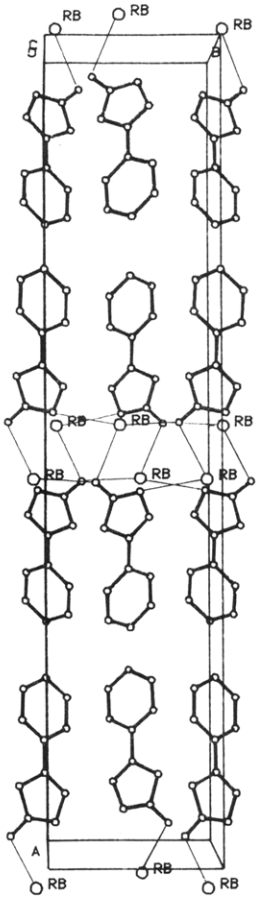

Figure 3. Ball-and-stick drawing of the packing of Rb^+ salt. (For purpose of clarity, metal atoms are represented by large open circle and others (C, N, O) by small open circles.)

There is no evident correlation between the X-ray intramolecular structures and the salt behavior under heterogeneous alkylation because they have very similar ge-

Table III. Intermolecular Contacts in the Ag^+ and Rb^+ Salt Packings

atom 1	atom 2	distance, Å	symmetry N/O[a]	translations[b]
Ag^+	N(4)	2.09	1	0 0 0
	W(1)	2.12	1	0 0 0
W(2)	O(6)	2.82	1	0 0 0
O(6)	W(2)	2.86	4	0 2 0
Rb^+	O(6)	2.87	3	0 -1 0
	O(6)	3.06	1	0 0 0
	O(6)	3.10	5	0 0 0
	N(4)	2.94	3	0 0 0
	N(4)	3.03	1	0 0 0
	N(3)	3.04	3	0 0 0
	N(3)	3.13	5	0 0 1

[a] Symmetry N/O are as follows for Ag^+: (1) X, Y, Z; (2) $-X, {}^1/_2 + Y, {}^1/_2 - Z$; (3) $-X, -Y, -Z$; (4) $X, {}^1/_2 - Y, {}^1/_2 + Z$. For Rb^+ they are as follows: (1) X, Y, Z; (2) ${}^1/_2 + X, {}^1/_2 - Y, -Z$; (3) $-X, {}^1/_2 + Y, {}^1/_2 - Z$; (4) ${}^1/_2 - X, -Y, {}^1/_2 + Z$; (5) $-X, -Y, -Z$; (6) ${}^1/_2 - X, {}^1/_2 + Y, Z$; (7) $X, {}^1/_2 - Y, {}^1/_2 + Z$; (8) ${}^1/_2 + X, Y, {}^1/_2 - Z$. [b] The translations are along a, b and c, respectively.

ometries and electronic properties in the heterocyclic target rings. However the packings are completely different (Figures 2 and 3, stereoviews are given as supplementary material): (1) According to space group considerations, the molecules adopt head-to-tail (Ag^+) and head-to-head (Rb^+) arrangements.

(2) The Ag^+ salt displays a very strong interaction between the N(4) nitrogen atom and the Ag^+ cation; d(N(4)···Ag^+ = 2.09 Å. The silver atom is located in the mean plane of the oxadiazolone ring (deviation out of the best plane of atoms C(1) to O(6) = 0.16 Å), aligned with the lone pair of the N(4) atom. This value illustrates the strong affinity of silver(I) for amidic nitrogen atoms. This short distance can be compared to a similar N···Ag^+ bond of 2.08 Å observed in the silver nitrate complex of methylthymine.[12] The other Ag···N distances compiled for N-ligand complexes range from 2.2 to 2.7 Å.[13] The Ag^+ cation is also linked to the molecule water labeled W(1) and displays a linear coordination (N(4)–Ag–W(1) = 177°). This W(1) molecule is tightly linked to the Ag^+ cation (2.12 Å), and the hydrogen atoms can be easily observed on a Fourier difference map despite the fact they lie in the neighborhood of the strong Ag^+ electronic density. The hydrogen-bond network is rather simple and constituted by weaker interactions between the O(6) atoms and the W(2) molecules. This complete hydrogen-bond network involves the molecules ...(4 0 2 -n)...(1 0 0 (-n + 1))...(4 0 2 (-n + 1))..., leading to an infinite network along the c axis (Table III; Figure 2).

From these observations, it is clear that the silver salt can be considered as a tight ion pair in which a strong masking effect of the cation over the N(4) atom occurs. This proximity of Ag^+ and N(4) leaves the O(6) oxygen atom free for alkylation. The lone pair of the N(3) nitrogen atom, which lies close to the plane of the phenyl ring, is the next accessible position (Figure 4). However, it is subject to steric hindrance by the phenyl group; only a reagent such as CH_3I is small enough to alkylate the N(3) atom. In all other cases, only the free O(6) oxygen atom can be alkylated.

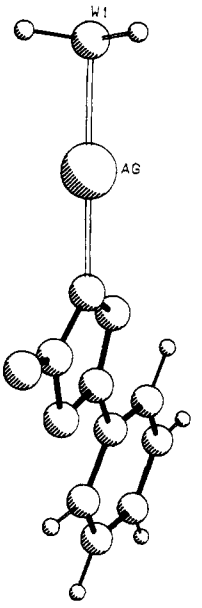

Figure 4. Enclosure sphere of the neighboring atoms around Ag^+ (the corresponding distances are reported in Table III).

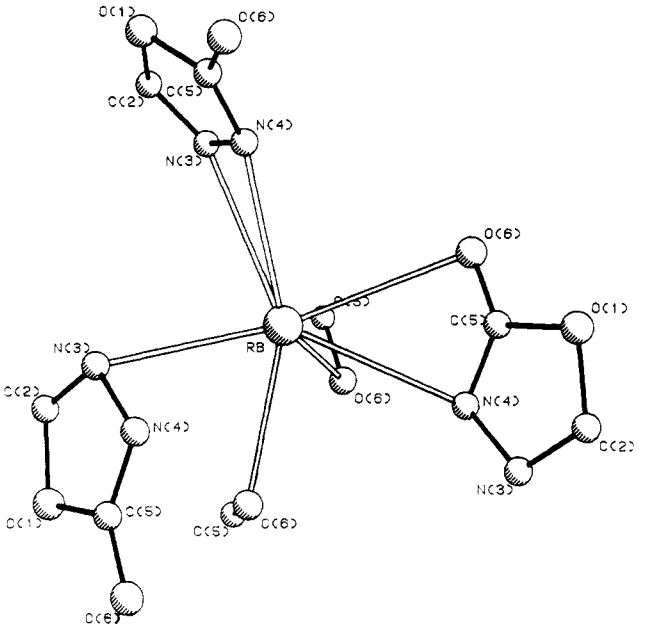

Figure 5. Enclosure sphere of the neighboring atoms around Rb^+ (the corresponding distances are reported in Table III).

(3) A very different situation occurs in the Rb^+ salt packing: The cation is less stabilized by coulombian interactions but with numerous contacts (Table III, Figures 3 and 5), involving all the heteroatoms of the anion. The minimum distance is d(Rb···O(6)) = 2.87 Å; the two others that can be considered as short contacts are d(Rb···N(3)) = 3.04 Å and d(Rb···N(4)) = 2.94 Å. The Rb^+ cation is also linked to another O(6) atom of a differently symmetry related anion, d'(Rb···O(6)) = 3.10 Å. At the opposite to the Ag^+ salt, there is no molecule of solvent in the packing.

The most interesting feature of the Rb^+ salt packing is a bilayer stacking of the cations and anions in planes parallel to the face A. Each pair of rubidium-containing planes (edge-viewed in Figure 3) are located around A = 0 (and $A = {}^1/_2$ by symmetry), with a 2.3-Å space between the stacked planes of the pair. A single plane contains zig-zag ribbons of rubidium in such a way that a particular

(12) Guay, F.; Beauchamp, A. I. *J. Am. Chem. Soc.* **1979**, *101*, 6260–6263. See also a catena(methyl-adenine) complex with an Ag···N distance of 2.15 Å: Gagnon, C.; Beauchamp, A. I. *Acta Crystallogr., Sect. B* **1977**, *B33*, 1448–1454.

(13) (a) Ansell, G. B. *J. Chem. Soc., Perkin Trans. 2* **1976**, 104–106. (b) Nelson, S. M.; McFall, S. G.; Drew, M. G. B.; Othman, A. H.; Masson, N. B. *J. Chem. Soc., Chem. Commun.* **1977**, 167–168. (c) Cook, D. S.; Turner, M. F. *J. Chem. Soc., Perkin Trans. 2* **1976**, 1379–1383. (d) Francisco, R. H. P.; Mascarehnas, Y. P.; Lechat, J. R. *Acta Crystallogr., Sect. B* **1979**, *35*, 177–178.

rubidium is surrounded by three others in a shell of radius 4.0 Å < r < 4.5 Å: d(Rb···Rb(5 0 0 1)) = 4.03 Å, d(Rb···Rb(3 0 0 0)) = 4.32 Å, and d(Rb···Rb(7 0 1 1)) = 4.42 Å.[14] All the short distances obtained from the packings are reported in Table III along with the connecting symmetry operators to be applied on the second atom.

This very different situation of the cation short contacts with respect to the Ag^+ salt leads now to a shielding effect not selectively distributed (the short distances are now in the range 2.8–3.2 Å) over all the alkylation sites. This could be a good explanation of the nonreactivity of the rubidium salt when the solid state is implicated in the alkylation process (heterogeneous dispersion in CH_2Cl_2). Moreover, this shielding is enhanced by the aggregation of the rubidium atoms in meridian planes, which acts as an additional steric protection against the alkylating reagent.

Conclusion

The present study shows a good agreement between the packing structures of two solid salts of ambident anions of the 2-phenyl-1,3,4-oxadiazol-5(4*H*)-one and their reactivity in alkylation reaction under heterogeneous conditions: (1) In the Ag^+ salt, where a strong ion pair exists, the O(6) oxygen atom (and, to a lesser extent, the N(3) nitrogen atom) remains unprotected and thus can be alkylated with a high selectivity. (2) In the Rb^+ salt, a widely distributed shielding effect of different, symmetrically related cations, occurs; all the atoms of the anion are affected by this shielding and the anion cannot be alkylated at any position.

Thus, the steric hindrance of the cation over the rest of the molecule can be considered as the leading factor in the control of the regioselectivity observed *in heterogeneous conditions*. These results strongly suggest that the same kind of steric effect might also explain the behavior of the other alkaline salts of the 2-phenyl-1,3,4-oxadiazol-5-(4*H*)-one, which is the same as that of the rubidium salt.

Registry No. 2-Phenyl-1,3,4-oxadiazol-5(4*H*)-one silver salt, 98218-22-5; 2-phenyl-1,3,4-oxadiazol-5(4*H*)-one rubidium salt, 98218-23-6.

Supplementary Material Available: Tables containing positional parameters with anisotropic thermal u factors, distances, and angles and stereorepresentations of Figures 2 and 3 (6 pages). Structure factor tables are available from the authors. Ordering information is given on any current masthead page.

(14) The symbolic of symmetry operations to be applied on the second atom is given in Table III.

Electrocyclization and Cyclooligomerization Reactions of 2,7-Dimethyl-2,3,5,6-octatetraene with Ni(0) and Ni(II) Complexes

Daniel J. Pasto* and Nai-Zhong Huang

Department of Chemistry, University of Notre Dame, Notre Dame, Indiana 46556

Received May 1, 1985

The reactions of 2,7-dimethyl-2,3,5,6-octatetraene (DMOT) with several Ni(0) and Ni(II) complexes have been investigated. The results indicate that the product(s) produced depends on the nature of the ligands attached to the nickel and the oxidation state of the nickel atom. The reaction of DMOT with tris(triphenylphosphine)nickel(0) [$(TPP)_3Ni$] quantitatively produces the cyclic trimer **3**. In contrast, the reaction of DMOT with bis(cyclooctadiene)nickel(0) [$(COD)_2Ni$] results in the electrocyclic ring closure to **4** and the formation of the cyclic dimer **5**. The reaction of DMOT with a mixture of $(COD)_2Ni$ and (COD)(TPP)Ni results in the formation of a mixture of **3** and **5**. The electrocyclic ring closure of DMOT to **4** is catalyzed by bis(triphenylphosphine)nickel dibromide, but not by bis(triethylphosphine)nickel dibromide. A general mechanism is proposed for the reactions of DMOT with the Ni(0) complexes.

In an attempt to prepare allenylnickel complexes by the oxidative insertion of a Ni(0) complex with substituted propargyl chlorides, we discovered an unusually facile formation of 3,4-bis(alkylidene)cyclobutenes **1**.[1] A reasonable mechanism was thought to involve the formation of intermediate substituted 1,2,4,5-tetraenes **2**. Prior studies in our[2] and other laboratories[3] had shown that the electrocyclic ring closure of **2** to **1** occurred thermally, however, under much more vigorous conditions than those employed for the formation of **1** in the reactions of the Ni(0) complexes with the substituted propargyl chlorides.

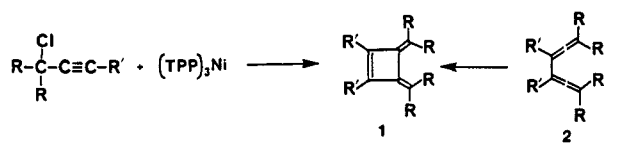

This suggested that the conversion of **2** to **1** was catalyzed by some Ni species present in the reaction mixture. In a continuation of our studies of the reactions of substituted allenes with Ni(0) complexes[4] we have now studied the reactions of 2,7-dimethyl-2,3,5,6-octatetraene (DMOT) with Ni(0) and Ni(II) complexes.

Results and Discussion

The reaction of DMOT with $(TPP)_3Ni$ at room temperature in toluene-d_8 results in the rapid (<3 h) and quantitative (by NMR) formation of the cyclic trimer **3**. The ^1H and ^{13}C NMR spectra suggested that the product was a trimer of DMOT; although the mass spectrum showed only a very weak peak at m/e 402, the most intense peak in the spectrum appearing at m/e 268 (a dimeric structure of DMOT). The vinyl hydrogen region of the ^1H NMR spectrum of **3** showed one set of AB doublets,

(1) Pasto, D. J.; Mitra, D. K. *J. Org. Chem.* **1982**, *47*, 1381.
(2) Pasto, D. J.; Waterhouse, A., unpublished observations.
(3) Skattebol, L.; Solomon, S. *J. Am. Chem. Soc.* **1965**, *87*, 4506.
(4) (a) Pasto, D. J.; Huang, N.-Z. *Organometallics* **1985**, *4*, 1386. (b) *J. Am. Chem. Soc.* **1985**, *107*, 3160.

0022-3263/85/1950-4465$01.50/0